IAI
Journals.ASM.org

Expansion of Paneth Cell Population in Response to Enteric *Salmonella enterica* Serovar Typhimurium Infection

Nadine R. Martinez Rodriguez,[a] Marjannie D. Eloi,[a] Alexandria Huynh,[a] Teresa Dominguez,[a] Annie H. Cheung Lam,[a] Dayana Carcamo-Molina,[a] Zeina Naser,[a] Robert Desharnais,[a] Nita H. Salzman,[b] and Edith Porter[a]

Department of Biological Sciences, California State University Los Angeles, Los Angeles, California, USA,[a] and Department of Pediatrics, Division of Gastroenterology, Children's Research Institute, Medical College of Wisconsin, Milwaukee, Wisconsin, USA[b]

Paneth cells residing at the base of the small intestinal crypts contribute to the mucosal intestinal first line defense by secreting granules filled with antimicrobial polypeptides including lysozyme. These cells derive from the columnar intestinal stem cell located at position 0 and the transit amplifying cell located at position +4 in the crypts. We have previously shown that *Salmonella enterica* serovar Typhimurium (ST), a leading cause of gastrointestinal infections in humans, effects an overall reduction of lysozyme in the small intestine. To extend this work, we examined small-intestinal tissue sections at various time points after ST infection to quantify and localize expression of lysozyme and assess Paneth cell abundance, apoptosis, and the expression of Paneth cell differentiation markers. In response to infection with ST, the intestinal Paneth cell-specific lysozyme content, the number of lysozyme-positive Paneth cells, and the number of granules per Paneth cell decreased. However, this was accompanied by increases in the total number of Paneth cells and the frequency of mitotic events in crypts, by increased staining for the proliferation marker PCNA, primarily at the crypt side walls where the transit amplifying cell resides and not at the crypt base, and by apoptotic events in villi. Furthermore, we found a time-dependent upregulation of first β-catenin, followed by EphB3, and lastly Sox9 in response to ST, which was not observed after infection with a *Salmonella* pathogenicity island 1 mutant deficient in type III secretion. Our data strongly suggest that, in response to ST infection, a Paneth cell differentiation program is initiated that leads to an expansion of the Paneth cell population and that the transit amplifying cell is likely the main progenitor responder. Infection-induced expansion of the Paneth cell population may represent an acute intestinal inflammatory response similar to neutrophilia in systemic infection.

Innate mucosal immunity represents the first line of defense against infection by preventing microbes from crossing the gut lining and invading the bloodstream. Paneth cells, located at the base of small intestinal crypts, contribute to the mucosal defense mechanism in the small intestine through the secretion of granules filled with antimicrobial (poly)peptides such as lysozyme, phospholipase A2, defensins (called cryptdins in mice), and RegIIIγ (12, 42, 44, 51). Lysozyme is a bimodal polypeptide of approximately 14 kDa that hydrolyzes peptidoglycan (20) and also directly disrupts membranes, similar to antimicrobial peptides (29). In mice, two lysozyme genes are transcribed (27): one in myeloid cells (M lysozyme) and one in epithelial cells, in particular Paneth cells (P lysozyme). These two lysozymes share 92% homology but differ in their net charge with P lysozyme being more positively charged than M lysozyme (37).

In the small intestine, the intestinal stem cell located in the crypts gives rise to Paneth cells, as well as enterocytes, goblet cells, and enteroendocrine cells (55), as well as the recently discovered opioid producing tuft cells (24). Upon differentiation, Paneth cells remain in the crypts, while the other cell types migrate to the villi. Originally, the intestinal stem cell was localized to a position +4 in the crypts (46, 54, 56). However, recent research by Barker et al. (6) provided strong evidence that the intestinal stem cell is located in the base of the crypt and characterized by the expression of Lgr5, a leucine-rich repeat-containing G-protein-coupled orphan receptor. In agreement with the latter model, several groups have named the proliferating cells in position +4 transit amplifying cells, which proliferate more rapidly than the intestinal stem cell, with an average cell cycle of 12 to 13 h compared to the 24-h cycling time, respectively (4, 5, 15, 39). However, this controversy has not yet been resolved (47).

Activation and proliferation of the intestinal stem cell and subsequent differentiation into Paneth cells are thought to involve Wnt4 signaling inducing nuclear translocation of β-catenin and activation of the transcription factor Tcf4 (1, 34, 59, 60, 63) and eventually of EphB3 (9) and Sox9 (8, 21, 40), among other markers (61). Eph receptors are important for the development of tissue architecture (30). EphB3, which is predominantly expressed by Paneth cells in the small intestine (28), has been shown to be essential for Paneth cell positioning in the crypt (9). Sox9 is a HMG-box transcription factor and a downstream target of the Wnt/β-catenin/Tcf4 complex (10) and has been shown to be essential for Paneth cell (as well as goblet cell) development since disruption of the gene leads to a disappearance of Paneth cells (8, 18, 40). Other factors important for Paneth cell development have been recently identified including Lgr4, EGF3, and cdx2 (11, 14, 41).

Even though Paneth cells release an abundance of antimicro-

Received 9 July 2011 Returned for modification 9 August 2011
Accepted 7 October 2011
Published ahead of print 17 October 2011
Editor: B. A. McCormick
Address correspondence to Edith Porter, eporter@calstatela.edu, or Nita H. Salzman, nsalzman@mcw.edu.

doi:10.1128/IAI.05638-11

bial (poly)peptides into the intestinal lumen (3), pathogenic microorganisms are able to interfere with this barrier function. We previously showed that *Salmonella enterica* serovar Typhimurium (ST) can downregulate cryptdin and lysozyme production in mice (52), although it was unclear whether lysozyme reduction primarily involved P lysozyme or also affected M lysozyme. *Salmonella* infection can also lead to induction of proinflammatory programmed cell death (pyroptosis) in macrophages (19, 25) and apoptosis in enterocytes (64). Many of these virulence capabilities depend on expression of type III secretion systems, which are encoded on the *Salmonella* pathogenicity island (SPI) I and II. Studies with attenuated SPI mutants have been important to understand host pathogen interplay in *Salmonella* infections (33, 35).

In the present study, we investigated mechanisms by which *Salmonella* infection resulted in reduced intestinal lysozyme expression. We determined that loss of lysozyme expression was Paneth cell specific but not associated with Paneth cell apoptosis. Although there was evidence of villus epithelial apoptosis, enteric *Salmonella* infection triggered intestinal progenitor cell proliferation and the initiation of a Paneth cell differentiation program resulting in increases in Paneth cell numbers with decreased granule content. In contrast, an SPI mutant did not initiate Paneth cell expansion. Thus, we provide novel evidence that the expansion of Paneth cells is an acute intestinal immune response to infection with *Salmonella*.

MATERIALS AND METHODS

Mice. Female FvB wild-type mice were obtained from Taconic Laboratories and used between 5 and 6 weeks of age. Animals were housed under specific-pathogen-free conditions in the Medical College of Wisconsin Biomedical Resource Center vivarium. All animal work followed federal guidelines and was approved by the institutional review board of the Medical College of Wisconsin, Milwaukee, WI.

***Salmonella* infections and tissue preparations.** Animals were deprived of food overnight (18 h). Mice were inoculated with10^8 CFU of wild-type *Salmonella enterica* serovar Typhimurium (ST) strain 14028s, an SPI type III secretion system mutant TK93 (33, 52), or buffer only (sterile 0.2 M phosphate buffer [pH 8.0]), by oral gavage, as described previously (52). Mice were sacrificed postinoculation at times indicated. The terminal 1.5 cm of ileum of the small intestine was fixed in formalin and processed for histology. The remaining distal 15-cm portions of the small intestine were divided for protein extraction and RNA isolation and snap-frozen in liquid nitrogen.

For histology (hematoxylin and eosin [H&E] staining or immunofluorescence), formalin-fixed tissues were dehydrated through graded alcohols and xylene, embedded in paraffin, and cut into 4-μm sections, which were mounted onto glass slides for further use.

For protein extraction, whole gut tissue was homogenized and extracted with 60% acetonitrile, 5% acetic, and 0.1% trifluoroacetic acid supplemented with 7 μg of pepstatin/ml, an acidic protease inhibitor, overnight at 4°C under constant agitation. Extracts were clarified by high-speed centrifugation and dialyzed against 5% acetic acid and subsequently 0.01% acetic acid using a 10-kDa cutoff membrane (Mini Dialysis Unit; Pierce/Thermo Scientific, Rockford, IL). In some experiments, luminal washes with phosphate-buffered saline (PBS) were collected, clarified by high-speed centrifugation, and dialyzed as described above. Protein concentration was determined with the BCA protein assay kit according to the manufacturer's protocol (Pierce/Thermo Scientific).

Total RNA was isolated from snap-frozen tissue using Ultraspec reagent (Biotecx) and stored at 350 ng/μl in 70% ethanol-diethyl pyrocarbonate-water.

Western immunoblotting. P and M lysozymes were quantified in whole-gut tissue extracts by Western immunoblotting after acid-urea polyacrylamide gel electrophoresis (AU-PAGE) as described previously (17) using 10-cm wide by 10-cm long gels for enhanced protein separation, and rabbit polyclonal antibodies against M and P lysozymes diluted 1:500 (52). Recombinant M and P lysozymes, as well as crude protein extracts from mouse small intestinal crypts for P lysozyme (52) and mouse neutrophil extracts for M lysozyme, were used as standards. For the latter, mice were intraperitoneally injected with 2% thioglycolate and sacrificed 4 h later. Peritoneal exudates were collected, the cells were sedimented by centrifugation, and proteins were extracted from the cell pellets and dialyzed as described above for gut tissue extracts. The relative lysozyme levels were quantified by the Versadoc imaging system (Quantity One Software; Bio-Rad, Hercules, CA) comparing ratios of individual test sample signal densities (adjusted intensity/mm^2) to standard signal densities for each blot.

Immunofluorescence. Lysozyme expression in Paneth cells and myeloid cells was determined by immunofluorescence using formalin-fixed tissue sections, rabbit polyclonal antibodies against P and M lysozymes (generous gift from Tomas Ganz, University of California at Los Angeles), and Alexa Fluor 594 (red fluorescence)-conjugated chicken anti-rabbit IgG. All steps were performed at room temperature unless stated otherwise. Slides were deparaffinized and rehydrated (45). To enhance immunoreactivity, antigen retrieval was performed by incubating slides in 10 mM sodium citrate (pH 6.0) for 30 min at 80°C (50). After cooling to room temperature, slides were incubated in 100 mM glycine for 5 min. Slides were blocked for 20 min (50 mM Tris-HCl, 150 mM NaCl, 1% ovalbumin, 0.2% gelatin, 0.05% Tween 20, and 0.4% fish gelatin) and then incubated overnight in a mixture of anti-P and anti-M lysozyme sera (each diluted 1:4,000 in 0.25% nonfat milk powder in PBS). The slides were then rinsed in Tris-buffered saline (TBS), followed by incubation for 1 h at 37°C with Alexa Fluor 594-conjugated chicken anti-rabbit IgG antibody (Molecular Probes, Eugene, CA) diluted 1:1,000 in 50 mM Tris-HCl. The slides were then washed in TBS supplemented with 0.05% Tween 20 and mounted (Gel Mount; Biomeda, Foster City, CA). The slides were coded and viewed under a Zeiss EPI 400 fluorescence microscope and Paneth cell and myeloid cells were independently enumerated by two observers in a blinded manner. For each tissue, 20-well preserved crypts along the longitudinal crypt-villus axis distributed over at least two different locations within the tissue sample were analyzed at ×400 magnification. Staining was performed twice, and the results were averaged. Images were taken using an Olympus Fluoview 500 microscope (Olympus, Center Valley, PA) in XY scan mode at ×400 magnification.

Quantification of apoptotic events. An apoptosis TUNEL (terminal deoxynucleotidyltransferase-mediated dUTP-biotin nick end labeling) detection kit was used with digoxigenin-labeled nucleotides and a fluorescein isothiocyanate-labeled antibody against digoxigenin (Chemicon, Temecula, CA). Small-intestinal tissue sections were deparaffinized and rehydrated as before, washed for 5 min in PBS, further processed according to the manufacturer's instructions, and counterstained with propidium iodide. The slides were coded and viewed using a Nikon Eclipse E400 fluorescence microscope (Nikon Instruments, Inc., Melville, NY). Apoptotic events represented by green fluorescent nuclei were independently enumerated in 40 intact intestinal villi and corresponding crypts per individual mouse by two observers in a blinded manner. The images shown here were obtained by using an Olympus Fluoview 500 microscope in XY scan mode at ×400 magnification.

Enumeration of Paneth cells, Paneth cell granules, and mitotic events. H&E-stained tissue sections were analyzed with a Nikon Eclipse E400 phase-contrast microscope under oil immersion at ×1,000 magnification. The slides were coded and analyzed by two observers in a blinded manner. The number of granules/Paneth cell and the number of Paneth cells were recorded for 40 well-preserved crypts per individual mouse. The number of mitotic events was determined for three independent sections with 40 well-preserved crypts and associated villi per individual mouse.

Visualization of proliferation. Deparaffinized and rehydrated sections were transferred into 0.1 M sodium citrate buffer (pH 6.0) and

TABLE 1 qPCR primer sequences and expected product sizes

Product	Sequence (5′–3′)		Product size (bp)
	Forward	Reverse	
β-Actin	ACCCACACTGTGCCCATCTA	TCATGGATGCCACAGGATTC	350
β-Catenin	AAGGAAGCTTCCAGACATGC	AGCTTGCTCTCTTGATTGCC	398
Lgr5	AACGGTCCTGTGAGTCAACC	CTCCTGCTCTAAGGCACCAC	303
Sox9	GAGCAGCAGCAGCACTCCCC	GGCCGGCTGCGTGACTGTAG	148
EphB3	GTCCGGGCTCGCACAGTAGC	GCCATGGCGCTGCTTCCTGA	198

heated in a microwave oven for 15 min for improved antigen retrieval. Sections were blocked in 10% bovine serum albumin (BSA) in PBS for 1 h at room temperature and then incubated for 75 min at room temperature with monoclonal mouse anti-PCNA (Leica-Microsystems, Buffalo Grove, IL) diluted 1:100 in 1% BSA in PBS. After three washes with PBS supplemented with 0.15 M NaCl (pH 7.4), the sections were incubated for 1 h at room temperature with biotinylated horse anti-mouse IgG (Vector Laboratories, Burlingame, CA) diluted 1:250 in 1% BSA in PBS, followed by incubation with Texas Red avidin B (Vector Laboratories) diluted at 1:1,000 in 1% BSA in PBS for 1 h at room temperature. Nuclear counterstain was done with DAPI (4′,6′-diamidino-2-phenylindole; Roche Applied Science, Indianapolis, IN) at 1 μg/ml in 1% BSA in PBS for 15 min at room temperature. After a washing step as described above, the slides were mounted in Fluoro-Gel with Tris buffer (Electron Microscope Sciences). Pictures were taken with an Olympus IX81 confocal microscope at ×100 and ×400 magnifications. No PCNA was visualized in control reactions omitting the primary antibody.

Quantitative reverse transcription-PCR. Portions (5 μg) of RNA were reverse transcribed to cDNA using an iScript cDNA synthesis kit according to the manufacturer's instructions (Bio-Rad). SYBR green technology and a MyiQ instrument (Bio-Rad) were used for quantitative PCR (qPCR). Forward and reverse primers for Lgr5, EphB3, and Sox9 were designed using the NCBI Primer BLAST designing tool and the GI number of the gene of interest. Primer sequences for β-actin and β-catenin were taken from Takano et al. (57) and de Vries et al. (16), respectively. The sequences and expected product sizes for all primers are shown in Table 1. Primers were obtained from Invitrogen, Carlsbad, CA.

The real-time PCR mixture contained the following: 1 μl of cDNA template, 10 μl of Bio-Rad SYBR green Supermix, 2.5 μl of 3 μM concentrations of each forward and reverse primer, and 9 μl of nuclease-free water. The PCR conditions were as follows: 1 cycle of 3 min at 95°C; followed by 32 cycles of 30 s at 95°C, 20 s at 60°C, and 30 s at 72°C; and 1 final extension for 7 min at 72°C. To ascertain the purity of the product, melting curves were obtained after each run using the instrument's default program. In addition, PCR products were analyzed on ethidium bromide-stained 2% agarose gels and subjected to sequencing (City of Hope, Duarte, CA) to confirm target gene amplification according to routine molecular biology procedures. The increase or decrease in gene expression in ST-infected mice was calculated with MyiQ software using the $\Delta\Delta C_T$ method and β-actin for normalization.

Data analysis. Excel Microsoft Office 2003 was used to perform data calculations, and PASW version 18 was used for statistical analysis. Unless stated otherwise, a univariate two-factor analysis of variance (ANOVA) with treatment and time as the main factors and a time-treatment interaction term were used for calculating the statistical significance. *Post hoc* contrasts with a Bonferroni adjustment were used to compare the means for control and ST within each time period. The data were graphed with SigmaPlot version 9.0.

RESULTS

Lysozyme downregulation is Paneth cell specific. Our previous study showed that ST induced a downregulation of lysozyme in the small intestine (52). We investigated whether this effect was confined to Paneth cell lysozyme expression or whether it reflected a broader inhibition of innate immune defenses involving lysozyme expression by myeloid cells. Mice were inoculated with ST or buffer only; after 18 and 72 h, small-intestinal tissue sections were removed and analyzed by immunofluorescence and Western immunoblotting to assess lysozyme expression at the cellular (Fig. 1) and protein (Fig. 2) levels, respectively.

Compared to tissue sections from control mice (Fig. 1a and d), tissue sections from mice infected with ST (Fig. 1c and f) have reduced numbers of lysozyme-positive Paneth cells and reduced overall fluorescence intensity nearly to the levels of background staining (Fig. 1e). In phase contrast, Paneth cells from ST-infected mice appeared devoid of granules. The absence of lysozyme-positive cells in the lamina propria or submucosa suggests the absence of myeloid cell influx in infected or control mice at these time points.

We next evaluated the presence and quantity of P lysozyme and M lysozyme in whole-gut tissue extracts 18 and 72 h after infection (Fig. 2). P and M lysozyme antisera are cross-reactive; however, these two enzyme forms can be distinguished based on their charge differences (P lysozyme being more cationic), by using long AU gels that allowed electrophoretic separation of the two lysozymes. Figure 2a shows a representative Coomassie blue-stained AU-PAGE, demonstrating equal loading for the series of Western immunoblot experiments that were conducted. Figure 2b shows a representative Western immunoblot (top) and the corresponding analysis for P lysozyme intensities (bottom). The relative band intensities for P lysozyme were determined in triplicate for two independent animal experiments (summarized in Fig. 2c and d). We observed a statistically significant decrease of P lysozyme after infection with ST in both experiments ($P = 0.003$ and $P = 0.033$, respectively). Analysis of intestinal luminal washes did not yield detectable levels of P or M lysozyme at these time points (data not shown). These data argue against the possibility that decreases in P lysozyme are due to Paneth cell degranulation at these later time points in the course of the infection. M lysozyme was present in whole-gut tissue extracts, although at very low levels that could not be reliably quantified (Fig. 2b, top panel). This is consistent with the immunofluorescence analysis suggesting a lack of significant influx of myeloid cells at these time points and confirmed by the absence of notable inflammation in H&E-stained sections (data not shown). These data suggest that infection with ST results in a decrease in P lysozyme in the mouse gut, without measurable impact on M lysozyme.

***Salmonella* infection induces apoptosis in villus epithelium but not in the crypt base where Paneth cells are located.** ST has been shown to induce apoptosis in epithelial cells (64), suggesting that the loss of lysozyme positive Paneth cells could be due to

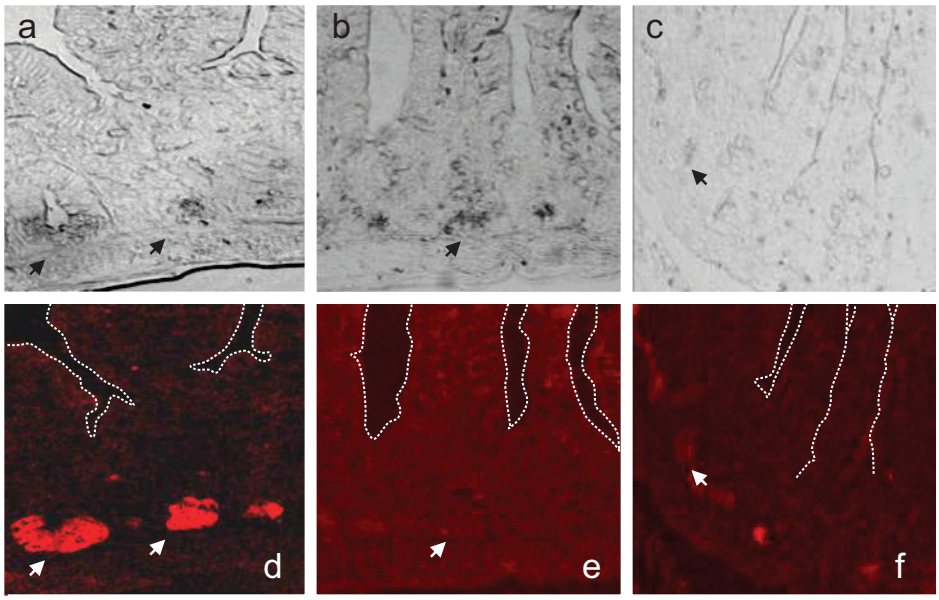

FIG 1 Loss of P lysozyme-positive Paneth cells in ST-infected mice. Small-intestinal tissue sections collected 72 h after infection were stained with rabbit polyclonal antibodies against M and P lysozymes and Alexa 594-conjugated chicken anti-rabbit antibodies. The top row shows phase-contrast images. The bottom row shows images from a fluorescence microscope. (a and d) Tissue sections from mice inoculated with PBS; (b and e) tissue sections from same mice stained without primary antibody; (c and f) tissue sections from mice infected with ST. Images were taken at ×400 magnification. Arrows point to Paneth cells. The white dashed lines in panels d to f trace villus-crypt axes.

ST-induced apoptosis. We therefore performed TUNEL staining on formalin-fixed tissue sections (Fig. 3). Representative images (Fig. 3) summarize the quantification of apoptotic events/crypt and villus. Apoptotic events were not evenly distributed within sections, with some crypts lacking apoptotic events and, therefore, data are shown here per 40 villus/crypt axes. Unexpectedly, there was a statistically significant increase of apoptotic cells in the villus and not in the crypt region in mouse small intestine 72 h after infection with ST compared to PBS-inoculated control mice of from 12 ± 1.98 to 26 ± 1.1 apoptotic cells/40 villi (means ± the standard error of the mean [SEM], $n = 5$ for control and $n = 4$ for ST; $P = 0.026$ in multivariate ANOVA with the Bonferroni adjustment for multiple comparisons).

***Salmonella* infection activates a differentiation program, resulting in an increase in Paneth cell numbers.** To assess the fate of Paneth cells independently from specific antimicrobial protein production in ST-infected mice, we enumerated characteristically pyramid-shaped Paneth cells and their granules in H&E-stained small-intestinal tissue sections obtained from mice 18 and 72 h after inoculation with PBS or ST (Fig. 4). The number of Paneth cells per crypt was statistically significantly increased in mice 18 and 72 h after infection with ST from 2.96 ± 0.15 to 5.24 ± 0.16 and from 3.22 ± 0.26 to 6.65 ± 0.21, respectively ($n = 3$, $P = <$ 0.0005; Fig. 4a). In contrast, the number of granules per Paneth cell was statistically significantly decreased in mice 72 h after infection with ST from 11.36 ± 0.63 to 7.71 ± 1.07 ($n = 3$, $P =$ 0.003; Fig. 4b). In addition, mitotic activity was increased in tissue sections from ST-infected mice compared to control mice (Fig. 5). Mitotic events per crypt significantly increased 18 and 72 h after infection, from 1.214 ± 0.056 to 1.506 ± 0.130 and from 1.863 ± 0.120 to 3.192 ± 0.262, respectively ($n = 9$ for all but for the control at 72 h, where $n = 7$ and $P < 0.0005$ for both comparisons; Fig. 5b). The majority of mitotic events localized to the crypt side wall around the region of position +4, where the transit amplifying cell is thought to reside, and not at the base of the crypt where the intestinal stem cell has been located. This was confirmed by the staining pattern of the nuclear proliferation marker PCNA (Fig. 5c). Although proliferating cells appeared at the base of the crypt in tissue sections obtained from control animals, substantially increased PCNA-positive cells appeared along the crypt side walls in tissue sections from ST-infected animals.

Increased mitotic events and increased expression of the nuclear proliferation marker PCNA accompanied by an increase in Paneth cell numbers in the crypts and apoptosis in the villi strongly suggested that intestinal progenitor cells underwent accelerated proliferation in response to ST infection, resulting in the generation of more Paneth cells, which were still immature and therefore less filled with granules and lysozyme. To corroborate this, we quantified the gene expression of β-catenin (a member of the Wnt signaling pathway involved in intestinal stem cell activation and initiation of differentiation), Lgr5 (a marker of the intestinal stem cell), and EphB3 and Sox9 to assess the induction of a Paneth cell development program (Fig. 6). The expression of β-actin was used to normalize mRNA expression. To detect early changes in gene expression in response to ST, we analyzed RNA obtained from tissues collected 1 and 4 h, in addition to 18 and 72 h, after infection or inoculation with buffer. Since the relative expression (RE) values varied over several orders of magnitude, we transformed the data to $\log_{10}$ RE for statistical analysis. The ANOVA for the $\log_2$ RE did not show significant main effects or a significant time-by-marker interaction. However, the overall intercept was significant ($P < 0.001$), indicating that, overall, infection with ST led to increased expression relative to the controls. The time points and markers showing significantly increased ex-

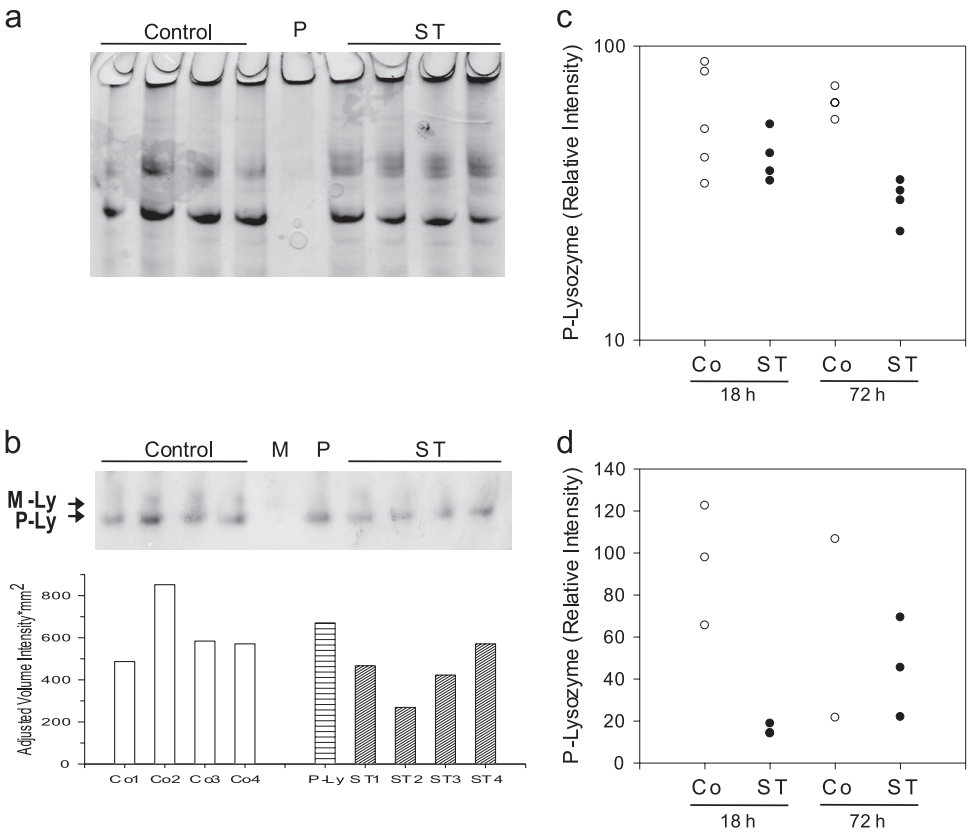

FIG 2 Reduction of P lysozyme in ST-infected mice. (a) Representative Coomassie blue-stained AU-PAGE from small-intestinal tissue protein extracts (12 μg/lane) 72 h after infection with ST or inoculation with PBS (control). Shown are extracts from four individual mice in each group. P, small-intestinal mucosal crypt extract (2.5 μg). (b) Western immunoblot with protein extract from the same mice (4.5 μg/lane, top) and corresponding intensity data for P lysozyme (bottom). M, neutrophil extract (1 μg) containing M lysozyme; P, same as described for panel a. Arrows point to M lysozyme (M-Ly) and P lysozyme (P-Ly). (c and d) Relative intensities for P lysozyme from two different animal experiments ($n = 4$ for panel c with the exception of Co 18 h, where $n = 5$; $n = 3$ for panel d, with the exception for ST 18 h where $n = 2$). The representative image shown in panel b is from the experiment whose results are shown in panel c. The data are expressed as relative P lysozyme intensities (test band intensity divided by intensity obtained from P lysozyme standard $\times$ 100). Shown are the averages of triplicate determinations of relative P lysozyme intensities from individual mice. Univariate two-factor ANOVAs of relative intensity show no significant differences due to time (18 h versus 72 h) and no significant interaction between time period and treatment for both experiments; however, there were significant differences between the control and ST groups, with $P = 0.003$ for the experiment shown in panel c and $P = 0.033$ for the experiment shown in panel d.

pression are indicated with an asterisk in Fig. 6. Specifically, ST-infected mice (Fig. 6, left panel) showed a significant short-term upregulation of β-catenin measurable 1 h after infection, followed 4 h after infection by a statistically significant increase of EphB3, and finally a significant increase of Sox9 expression measurable 72 h after infection. These results support that in response to ST the Paneth cell development program is activated and that the positioning of Paneth cells in the crypts precedes full differentiation. In contrast, at these time points we did not observe a significant change in Lgr5 expression, which suggests that the intestinal stem cell population did not significantly proliferate. To evaluate whether the observed changes are responses to an invasive pathogen rather than a reaction to the presence of microbial products, we repeated the experiment with an attenuated SPI1 *Salmonella* mutant strain (Fig. 6, right panel). In contrast to infection with wild-type ST, inoculation with the SPI1 mutant did not significantly increase the mRNA expression of markers associated with Wnt signaling and PC positioning and differentiation. Whereas Lgr5 expression was induced in SPI1-infected mice, β-catenin expression was unchanged and EphB3 and Sox9 expression were downregulated. Furthermore, we found that the number of Paneth cells did not increase after infection with the SPI1 mutant, in contrast to our findings for wild-type *Salmonella*. The average numbers of Paneth cells per crypt in control mice were 2.48 $\pm$ 0.47, 2.18 $\pm$ 0.36, 2.27 $\pm$ 0.25, and 2.61 $\pm$ 0.35 at 1, 4, 20.5, and 72 h after PBS inoculation, respectively. For the SPI mutant, the numbers of Paneth cells per crypt were 2.31 $\pm$ 0.23, 2.63 $\pm$ 0.14, 2.34 $\pm$ 0.56, and 2.89 $\pm$ 0.35 at 1, 4, 20.5, and 72 h after infection, respectively (compare this to 6.65 $\pm$ 0.21 Paneth cells per crypt in wild-type ST-infected mice). There was a statistically significant effect due to time showing slightly increased Paneth cell numbers per crypt at the 72-h time point from 2.48 $\pm$ 0.47 to 2.61 $\pm$ 0.35 in control mice and from 2.31 $\pm$ 0.23 to 2.89 $\pm$ 0.35 in SPI1-infected mice ($P = 0.047$), but treatment and interaction were not significant. Thus, Paneth cell expansion appears to be a targeted response to virulent ST infection correlating with the invasiveness of the strain.

DISCUSSION

In this study, we have shown that in response to infection with ST the intestinal P lysozyme content, the number of lysozyme-positive Paneth cells and their granule content decreased.

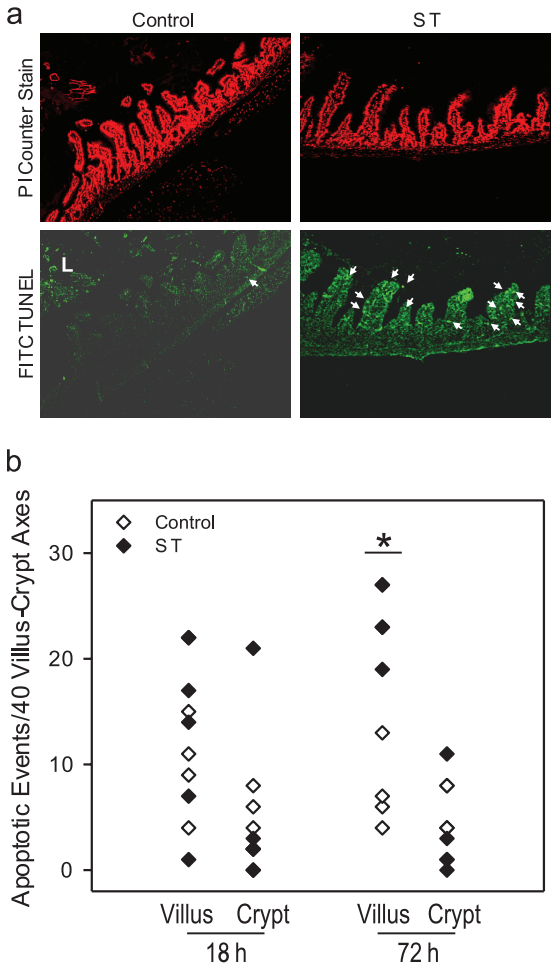

FIG 3 Increased apoptosis in villus epithelium in ST infected mice. (a) Representative image from confocal immunofluorescence microscopy of propidium iodide (PI) and TUNEL-stained tissue sections from small intestinal tissue at 72 h after ST infection at ×400 magnification. The arrow points to apoptotic events. L, luminal content not included in the analysis. (b) Summary showing mean apoptotic events per 40 villus-crypt axes. For all treatment groups, there were five mice, with the exception of ST 72 h, where $n = 4$. *, $P = 0.026$ in multivariate ANOVA with the Bonferroni adjustment for multiple comparisons.

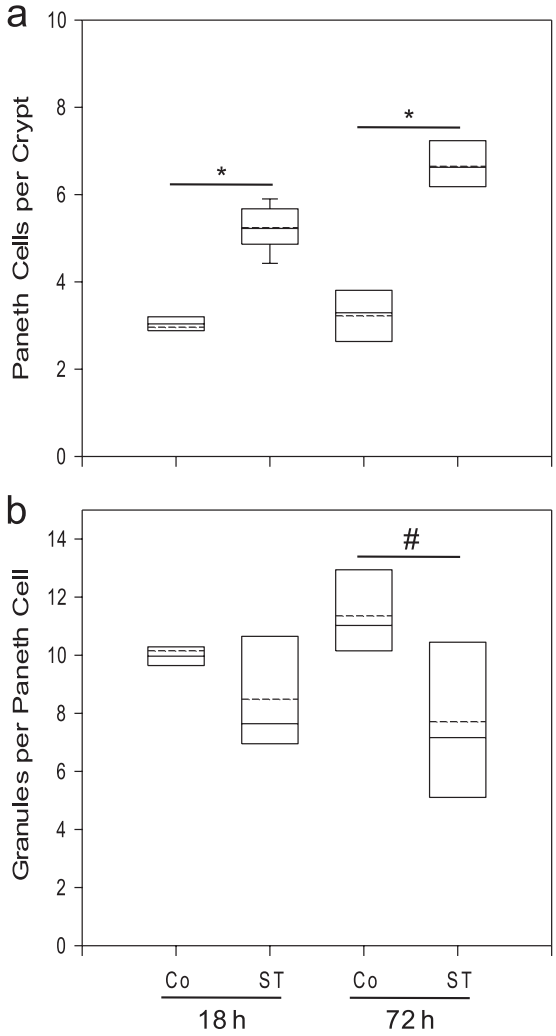

FIG 4 Increased Paneth cell numbers per crypt and decrease of granules per Paneth cell in ST-infected mice. Small-intestinal tissue sections were removed 18 and 72 h after infection with ST or inoculation with PBS (Co, control), formalin fixed, and H&E stained. Forty well-preserved crypts each were evaluated in two different sections for each mouse. (a) Paneth cell numbers per crypt; (b) granules per Paneth cell. The data are represented in box plots showing the 25th percentile closest to zero and the 75th percentile farthest from zero. The solid line within the box represents the median, and the dashed line represents the mean ($n = 3$). Error bars above and below represent the 90th and 10th percentiles, respectively, of each group. *, $P < 0.0005$; #, $P = 0.003$.

However, this was accompanied by an increase in the number of Paneth cells, the frequency of mitotic events in the crypts, and apoptotic events in the villi. Furthermore, we found a time-dependent induction of β-catenin, EphB3, and Sox9, genes involved in Paneth cell development, in response to ST, but not to an attenuated SPI1 mutant *Salmonella* strain.

Initially, we set out to determine which lysozyme form was reduced in ST-infected mice reflecting either a local (P lysozyme primarily affected) or a systemic impairment of the host barrier against ST (M lysozyme affected). We found that P lysozyme in small intestinal whole-gut tissue extracts was reduced after infection with ST. This decrease appeared less dramatic in the Western immunoblot analysis than in the immunofluorescence analysis. However, for Western immunoblot analysis whole-gut extracts were used, and changes at the individual Paneth cell (easily detectable using microscopic analysis of tissue sections) were likely overshadowed by the overall increase of PCs and an increase in the total granule numbers. We did not obtain evidence for an influx of myeloid cells in response to the bacterial infection, and M lysozyme protein was detected only in traces and inconsistently. In agreement with this, P lysozyme has been reported before to be the predominant lysozyme in normal mouse small intestine (37), and Barthel et al. have previously shown that a significant neutrophil influx in response to ST infection in mice occurs most consistently when mice have been pretreated prior to infection, for example, with streptomycin (7), which was not the case for our experimental protocol. The observed decrease in P lysozyme content could be the result of lysozyme degranulation into the intestinal lumen (3). However, we were unable to detect P ly-

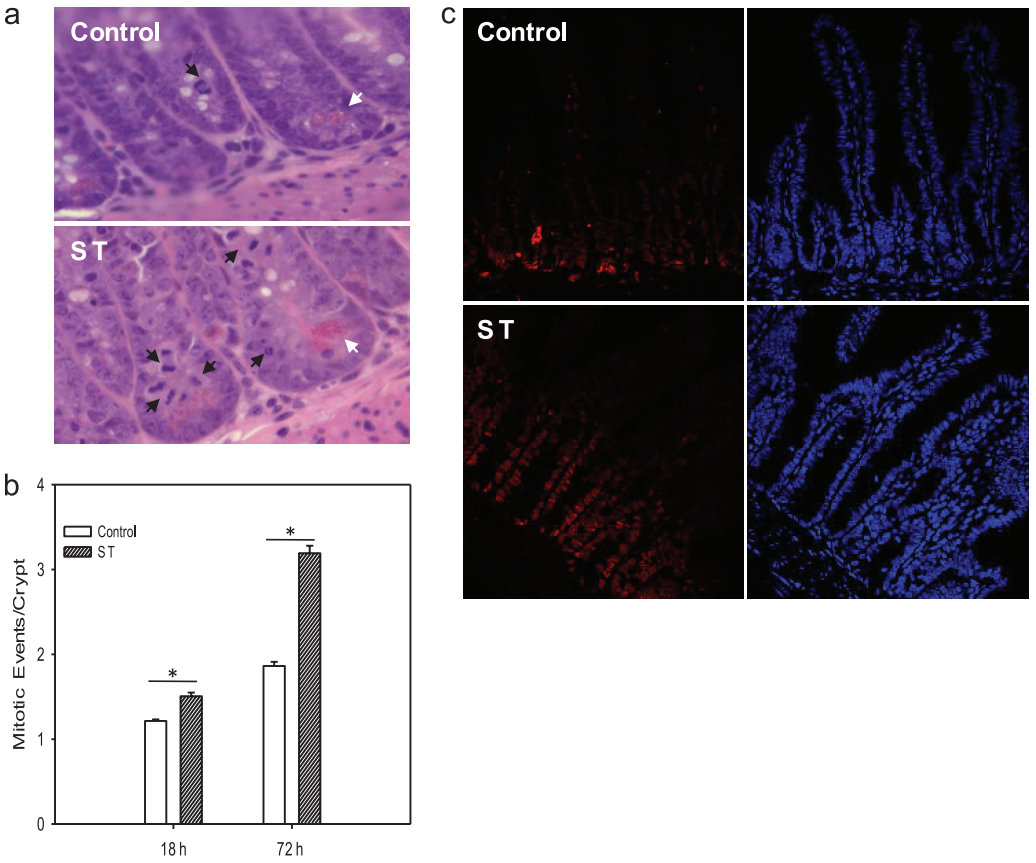

FIG 5 Increased mitotic events in ST-infected mice. (a) Representative H&E-stained small-intestinal sections obtained 72 h after inoculation with PBS (control) and ST. Black arrows point to mitotic events showing anaphase and prophase chromatin arrangements. White arrows point to Paneth cells. (b) For each mouse, the mitotic events of 40 crypts in three different sections were enumerated, except for the control at 72 h, where only two sections were evaluated. Shown are the means of mitotic events per crypt + the SEM, $n = 9$ for all but control at 72 h where $n = 7$. *, $P < 0.0005$ for both comparisons. (c) Same as panel a, but the tissue sections were probed for the proliferation marker PCNA (left panel) and stained with DAPI (right panel).

sozyme in the luminal washes at the time points analyzed. Considering that Rubio et al. observed replenishment of Paneth cell granules within 24 h after TLR9 ligand-induced degranulation (50) and the time frame of our experiment, we conclude that the originally observed decrease of lysozyme in ST-infected mice (52) results primarily from a decrease in Paneth cell derived lysozyme without involvement of myeloid cell and a local impairment to replenish the lysozyme pool.

We then hypothesized that ST may induce apoptosis of Paneth cells. However, we observed instead an increase in apoptotic events in the villi of small-intestinal sections obtained from ST-infected mice that was accompanied by an increased number of mitotic events in the crypt region and an expansion of Paneth cells. The Paneth cells contained fewer granules, accounting for the decrease in P lysozyme and the reduced numbers of lysozyme-positive Paneth cells in ST-infected mice. Even though ST has been shown to induce apoptosis in enterocytes (43, 64), the increased mitotic events and Paneth cell numbers appear to reflect rather an increased turnover rate of the small-intestinal epithelium (26). This is in agreement with Cliffe et al., who reported on crypt hyperplasia accompanied by increased apoptosis of enterocytes in chronic infection of mice with the nematode *Trichuris muris* (13).

Increased Paneth cell numbers in response to infection has been reported in a worm infection mouse model with *Trichinella spiralis* (31, 62). McConnell et al. demonstrated crypt cell hyperplasia in a bacterial mouse colitis model with *Citrobacter rodentium* (38). However, to the best of our knowledge, an expansion of the Paneth cell population has not been previously documented for ST or other enteric bacterial infections. Only very recently, Paneth cell hyperplasia has been associated with necrotizing enterocolitis in premature infants (48).

We found that an activation of the Wnt signaling pathway accompanied the expansion of the Paneth cell population in ST-infected mice. Similar findings were noted in a recent study by Liu et al. (36) and corroborated by reports of activation of Wnt signaling in response to helminth infections (32).

The increase of β-catenin expression occurred before the increase of EphB3 and Sox9 expression. This is consistent with Batlle et al. (9) and Blache et al. (10), who describe EphB3 and Sox9 as targets of Wnt signaling, respectively. We observed EphB3 upregulation prior to that of Sox9, which indicates that positioning of Paneth cells precedes its differentiation and full maturation into a secretory cell.

Sox9 expression was increased late during the course of the infection. This is in agreement with Formeister et al. (21), who demonstrate that Sox9 expression levels reciprocally influence

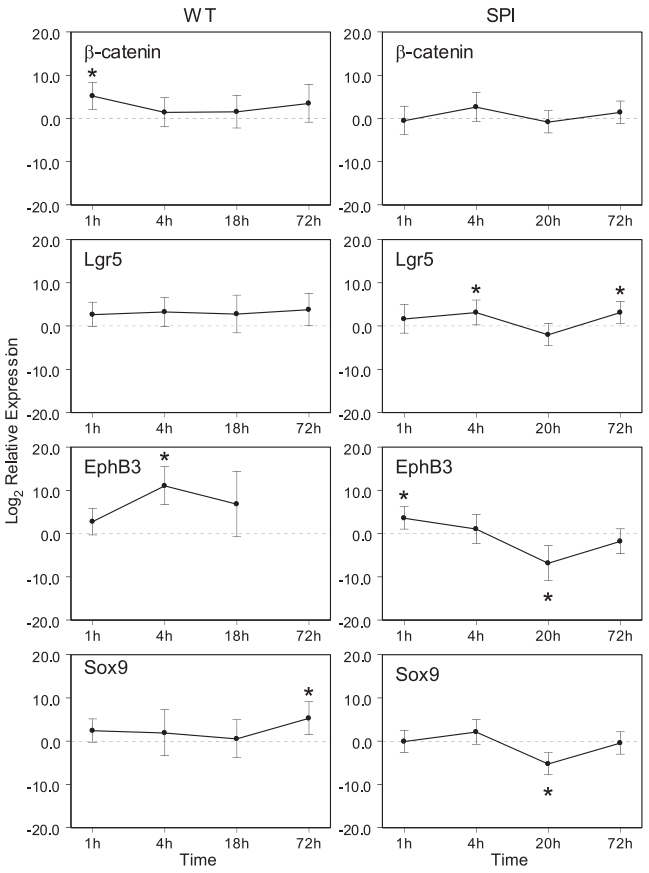

FIG 6 Gene expression of markers for Wnt signaling pathway, intestinal stem cells, and Paneth cell differentiation in mice infected with ST. Mice were infected with 10^8 ST or 10^8 SPI1 mutant or inoculated with PBS only. After various time points, the gene expression in infected mice relative to the expression in control mice was quantified using the $\Delta\Delta C_T$ method and β-actin as a reference gene (relative expression [RE]). Since the RE values varied over several orders of magnitude, data were transformed to the base 2 logarithm of the RE ($\log_2$ RE). The transformed data were analyzed as a two-factor ANOVA with time and marker as the fixed factors. The 95% confidence intervals were computed for the estimated marginal means of each treatment group. Since a value of $\log_2$ RE = 0 implies that the treatment and controls are equal, any confidence interval not containing zero was used to indicate statistical significance (marked by an asterisk [*] in the graphs). Each data point reflects duplicate measurements of at least three and up to five mice. (Left panels) Infection with wild-type ST (WT). EphB3 was not detectable at 72 h, and hence the relative expression could not be calculated. (Right panels) Infection with SPI1 mutant (SPI).

the proliferation in the intestinal crypt, with low Sox9 expression levels supporting but high Sox9 levels suppressing cell proliferation. Infection with an SPI1 mutant of ST induced a very different change in gene expression in the Paneth cell differentiation program. SPI1 mutant ST infection did not induce activation of β-catenin or increased expression of PC positioning and differentiation markers, nor did it induce an increase in the Paneth cell population. That SPI1 infection induced gene expression changes relative to the control was to be expected since SPI1 mutant strains have been shown to be unable to invade the intestinal epithelium but are able to translocate the epithelium at reduced numbers and persist within the phagolysosome (49). Based on these findings, we conclude that the observed Paneth cell expansion is not merely a response to microbial products but reflects a targeted response to bacterial invasion via the SPI1 type 3 secretion system.

We did not observe an increase in Lgr5 expression upon ST infection despite the activation of the Wnt signaling pathway, as reflected in the upregulation of β-catenin. This combined with the more frequent appearance of mitotic events and increased expression of the proliferation marker PCNA in the crypt side walls around position +4 suggests that the transit amplifying cells are the main responders to ST infection, not the columnar base intestinal stem cell. Recently, it has also been shown that transit amplifying cells constitute a distinct population of reserve stem cells in the intestine, providing an additional source of cellular renewal during injury (58). Increased transit amplifying cell proliferation has also been observed in other infection models (2) and recently in doxorubicin-induced intestinal injury (15). Furthermore, Garcia et al. have shown that Lgr5 may function as a negative regulator of Wnt pathway in the developing intestine (23). Thus, Lgr5 expression should not be increased when there is a demand for Wnt targets.

Considering that accelerated proliferation bears the danger of introduction of mutations, the intestinal stem cell may divide at a constant rate (5) and short-term responses may be regulated at the transit amplifying level. Hence, conciliating the discrepancies reported with respect to the location of the intestinal stem cell (47), we propose that in steady state the columnar base cells identified by Lgr5 give rise to all cell lineages but that in acute infection transit amplifying cells assume the main proliferative activity. A specialization of intestinal progenitor cell has been also recently suggested by Freeman (22).

In conclusion, we provide here strong evidence that in response to ST infection, activation of Wnt signaling initiates Paneth cell development with Paneth cell positioning in the crypts preceding its maturation. Infection-induced expansion of the Paneth cell population may represent an acute intestinal inflammatory response similar to neutrophilia during acute systemic inflammation, leading to the delivery of increased amounts of antimicrobials into the lumen upon full Paneth cell maturation. Future studies will be needed to dissect the underlying molecular events that drive transit amplifying cells to proliferate and enter a Paneth cell differentiation program and determine the significance of this proliferation in response to intestinal bacterial infection.

ACKNOWLEDGMENTS

This study was supported by CSU-LSAMP through NSF HRD-0331537 and the CSU office of the chancellor (N.R.M.R.), and MBRS-RISE 1 R25 GM61331 (M.D.E.), MARC GM 08228 (T.D.), P20 MD001824 (E.P.), and AI057757 (N.H.S.) from the National Institutes of Health.

We thank Andreas Baeumler, Charles L. Bevins, and Wolf-Dietrich Hardt for helpful discussions.

REFERENCES

1. **Andreu P, et al.** 2008. A genetic study of the role of the Wnt/β-catenin signaling in Paneth cell differentiation. Dev. Biol. **324**:288–296.
2. **Artis D, Potten CS, Else KJ, Finkelman FD, Grencis RK.** 1999. *Trichuris muris*: host intestinal epithelial cell hyperproliferation during chronic infection is regulated by interferon-gamma. Exp. Parasitol. **92**:144–153.
3. **Ayabe T, et al.** 2000. Secretion of microbicidal alpha-defensins by intestinal Paneth cells in response to bacteria. Nat. Immunol. **1**:113–118.

4. **Bach SP, Renehan AG, Potten CS.** 2000. Stem cells: the intestinal stem cell as a paradigm. Carcinogenesis **21**:469–476.
5. **Barker N, et al.** 2008. Very long-term self-renewal of small intestine, colon, and hair follicles from cycling Lgr5$^+$ stem cells. Cold Spring Harbor Symp. Quant. Biol. **73**:351–356.
6. **Barker N, et al.** 2007. Identification of stem cells in small intestine and colon by marker gene Lgr5. Nature **449**:1003–1007.
7. **Barthel M, et al.** 2003. Pretreatment of mice with streptomycin provides a *Salmonella enterica* serovar Typhimurium colitis model that allows analysis of both pathogen and host. Infect. Immun. **71**:2839–2858.
8. **Bastide P, et al.** 2007. Sox9 regulates cell proliferation and is required for Paneth cell differentiation in the intestinal epithelium. J. Cell Biol. **178**: 635–648.
9. **Batlle E, et al.** 2002. Beta-catenin and TCF mediate cell positioning in the intestinal epithelium by controlling the expression of EphB/ephrinB. Cell **111**:251–263.
10. **Blache P, et al.** 2004. SOX9 is an intestine crypt transcription factor, is regulated by the Wnt pathway, and represses the CDX2 and MUC2 genes. J. Cell Biol. **166**:37–47.
11. **Brodrick B, et al.** 2011. Fibroblast growth factor receptor-3 (FGFR-3) regulates expression of Paneth cell lineage-specific genes in intestinal epithelial cells through both TCF4/β-catenin-dependent and -independent signaling pathways. J. Biol. Chem. **286**:18515–18525.
12. **Cash HL, Whitham CV, Behrendt CL, Hooper LV.** 2006. Symbiotic bacteria direct expression of an intestinal bactericidal lectin. Science **313**: 1126–1130.
13. **Cliffe LJ, Potten CS, Booth CE, Grencis RK.** 2007. An increase in epithelial cell apoptosis is associated with chronic intestinal nematode infection. Infect. Immun. **75**:1556–1564.
14. **Crissey MA, et al.** 2011. Cdx2 levels modulate intestinal epithelium maturity and Paneth cell development. Gastroenterology **140**:517–528.
15. **Dekaney CM, Gulati AS, Garrison AP, Helmrath MA, Henning SJ.** 2009. Regeneration of intestinal stem/progenitor cells following doxorubicin treatment of mice. Am. J. Physiol. Gastrointest. Liver Physiol. **297**: G461–G470.
16. **De Vries WN, et al.** 2004. Maternal beta-catenin and E-cadherin in mouse development. Development **131**:4435–4445.
17. **Do TQ, et al.** 2008. Lipids including cholesteryl linoleate and cholesteryl arachidonate contribute to the inherent antibacterial activity of human nasal fluid. J. Immunol. **181**:4177–4187.
18. **Fernandez MI, et al.** 2008. Maturation of Paneth cells induces the refractory state of newborn mice to *Shigella* infection. J. Immunol. **180**: 4924–4930.
19. **Fink SL, Cookson BT.** 2007. Pyroptosis and host cell death responses during *Salmonella* infection. Cell Microbiol. **9**:2562–2570.
20. **Fleming A.** 1922. On a remarkable bacteriolytic element found in tissues and secretions. Proc. R. Soc. Lond. B Biol. Sci. **93**:306–317.
21. **Formeister EJ, et al.** 2009. Distinct SOX9 levels differentially mark stem/progenitor populations and enteroendocrine cells of the small intestine epithelium. Am. J. Physiol. Gastrointest. Liver Physiol. **296**: G1108–G1118.
22. **Freeman HJ.** 2008. Crypt region localization of intestinal stem cells in adults. World J. Gastroenterol. **14**:7160–7162.
23. **Garcia MI, et al.** 2009. LGR5 deficiency deregulates Wnt signaling and leads to precocious Paneth cell differentiation in the fetal intestine. Dev. Biol. **331**:58–67.
24. **Gerbe F, et al.** 2011. Distinct ATOH1 and Neurog3 requirements define tuft cells as a new secretory cell type in the intestinal epithelium. J. Cell Biol. **192**:767–780.
25. **Guiney DG.** 2005. The role of host cell death in *Salmonella* infections. Curr. Top. Microbiol. Immunol. **289**:131–150.
26. **Hall PA, Coates PJ, Ansari B, Hopwood D.** 1994. Regulation of cell number in the mammalian gastrointestinal tract: the importance of apoptosis. J. Cell Sci. **107**(Pt 12):3569–3577.
27. **Hammer MF, Wilson AC.** 1987. Regulatory and structural genes for lysozymes of mice. Genetics **115**:521–533.
28. **Holmberg J, et al.** 2006. EphB receptors coordinate migration and proliferation in the intestinal stem cell niche. Cell **125**:1151–1163.
29. **Ibrahim HR, Thomas U, Pellegrini A.** 2001. A helix-loop-helix peptide at the upper lip of the active site cleft of lysozyme confers potent antimicrobial activity with membrane permeabilization action. J. Biol. Chem. **276**: 43767–43774.
30. **Islam S, Loizides AM, Fialkovich JJ, Grand RJ, Montgomery RK.** 2010. Developmental expression of Eph and ephrin family genes in mammalian small intestine. Dig. Dis. Sci. **59**:2478–2488.
31. **Kamal M, Dehlawi MS, Brunet LR, Wakelin D.** 2002. Paneth and intermediate cell hyperplasia induced in mice by helminth infections. Parasitology **125**:275–281.
32. **Kim DM, et al.** 2009. Gene expression profiling in mouse liver infected with *Clonorchis sinensis* metacercariae. Parasitol. Res. **106**:269–278.
33. **Kimbrough TG, Miller SI.** 2000. Contribution of *Salmonella typhimurium* type III secretion components to needle complex formation. Proc. Natl. Acad. Sci. U. S. A. **97**:11008–11013.
34. **Koslowski MJ, et al.** 2009. Genetic variants of Wnt transcription factor TCF-4 (TCF7L2) putative promoter region are associated with small intestinal Crohn's disease. PLoS One **4**:e4496.
35. **Lee VT, Schneewind O.** 1999. Type III secretion machines and the pathogenesis of enteric infections caused by *Yersinia* and *Salmonella* spp. Immunol. Rev. **168**:241–255.
36. **Liu X, Lu R, Wu S, Sun J.** 2010. *Salmonella* regulation of intestinal stem cells through the Wnt/β-catenin pathway. FEBS Lett. **584**:911–916.
37. **Markart P, et al.** 2004. Comparison of the microbicidal and muramidase activities of mouse lysozyme M and P. Biochem. J. **380**:385–392.
38. **McConnell BB, Klapproth JM, Sasaki M, Nandan MO, Yang VW.** 2008. Kruppel-like factor 5 mediates transmissible murine colonic hyperplasia caused by *Citrobacter rodentium* infection. Gastroenterology **134**: 1007–1016.
39. **Montgomery RK, Breault DT.** 2008. Small intestinal stem cell markers. J. Anat. **213**:52–58.
40. **Mori-Akiyama Y, et al.** 2007. SOX9 is required for the differentiation of Paneth cells in the intestinal epithelium. Gastroenterology **133**:539–546.
41. **Mustata RC, et al.** 2011. Lgr4 is required for Paneth cell differentiation and maintenance of intestinal stem cells ex vivo. EMBO Rep. **12**:558–564.
42. **Ouellette AJ.** 2011. Paneth cell alpha-defensins in enteric innate immunity. Cell Mol. Life Sci. **68**:2215–2229.
43. **Paesold G, Guiney DG, Eckmann L, Kagnoff MF.** 2002. Genes in the *Salmonella* pathogenicity island 2 and the Salmonella virulence plasmid are essential for Salmonella-induced apoptosis in intestinal epithelial cells. Cell Microbiol. **4**:771–781.
44. **Porter EM, Bevins CL, Ghosh D, Ganz T.** 2002. The multifaceted Paneth cell. Cell Mol. Life Sci. **59**:156–170.
45. **Porter EM, Liu L, Oren A, Anton PA, Ganz T.** 1997. Localization of human intestinal defensin 5 in Paneth cell granules. Infect. Immun. **65**: 2389–2395.
46. **Potten CS, et al.** 2003. Identification of a putative intestinal stem cell and early lineage marker, musashi-1. Differentiation **71**:28–41.
47. **Potten CS, Gandara R, Mahida YR, Loeffler M, Wright NA.** 2009. The stem cells of small intestinal crypts: where are they? Cell Prolif. **42**: 731–750.
48. **Puiman PJ, et al.** 2011. Paneth cell hyperplasia and metaplasia in necrotizing enterocolitis. Pediatr. Res. **69**:217–223.
49. **Radtke AL, Wilson JW, Sarker S, Nickerson CA.** 2010. Analysis of interactions of *Salmonella* type three secretion mutants with 3-D intestinal epithelial cells. PLoS One **5**:e15750.
50. **Rumio C, et al.** 2004. Degranulation of Paneth cells via Toll-like receptor 9. Am. J. Pathol. **165**:373–381.
51. **Salzman NH.** 2008. Defensins versus bacteria: not just antibiotics anymore. Gastroenterology **134**:2174–2177.
52. **Salzman NH, et al.** 2003. Enteric *Salmonella* infection inhibits Paneth cell antimicrobial peptide expression. Infect. Immun. **71**:1109–1115.
53. Reference deleted.
54. **Scoville DH, Sato T, He XC, Li L.** 2008. Current view: intestinal stem cells and signaling. Gastroenterology **134**:849–864.
55. **Simon-Assmann P, Turck N, Sidhoum-Jenny M, Gradwohl G, Kedinger M.** 2007. In vitro models of intestinal epithelial cell differentiation. Cell Biol. Toxicol. **23**:241–256.
56. **Stappenbeck TS, Wong MH, Saam JR, Mysorekar IU, Gordon JI.** 1998. Notes from some crypt watchers: regulation of renewal in the mouse intestinal epithelium. Curr. Opin. Cell Biol. **10**:702–709.
57. **Takano-Maruyama M, et al.** 2006. Foxl1-deficient mice exhibit aberrant epithelial cell positioning resulting from dysregulated EphB/EphrinB expression in the small intestine. Am. J. Physiol. Gastrointest. Liver Physiol. **291**:G163–G170.
58. **Tian H, et al.** 2010. A reserve stem cell population in small intestine renders Lgr5-positive cells dispensable. Nature **478**:255–259.

59. **van der Flier LG, et al.** 2007. The intestinal Wnt/TCF signature. Gastroenterology **132**:628–632.
60. **van Es JH, et al.** 2005. Wnt signaling induces maturation of Paneth cells in intestinal crypts. Nat. Cell Biol. **7**:381–386.
61. **Vidrich A, et al.** 2009. Fibroblast growth factor receptor-3 regulates Paneth cell lineage allocation and accrual of epithelial stem cells during murine intestinal development. Am. J. Physiol. Gastrointest. Liver Physiol. **297**:G168–G178.
62. **Walsh R, Seth R, Behnke J, Potten CS, Mahida YR.** 2009. Epithelial stem cell-related alterations in *Trichinella spiralis*-infected small intestine. Cell Prolif. **42**:394–403.
63. **Wehkamp J, et al.** 2007. The Paneth cell alpha-defensin deficiency of ileal Crohn's disease is linked to Wnt/Tcf-4. J. Immunol. **179**:3109–3118.
64. **Zeng H, et al.** 2006. Flagellin/TLR5 responses in epithelia reveal intertwined activation of inflammatory and apoptotic pathways. Am. J. Physiol. Gastrointest. Liver Physiol. **290**:G96–G108.